Journal of Geo-Energy and Environment
http://dx.doi.org/10.62762/JGEE.2025.781750

RESEARCH ARTICLE

Organic Geochemical Characteristics and Thermal Evolution Characteristics of Paleogene to Neogene Source Rocks in Mangai Area, Qaidam Basin

Shiling Shi[1,2], **Changan Shan**[1,2,*], **Ze Zhao**[3], **Yue Fei**[1,2] **and Jiaqi Zhang**[1,2]

[1] School of Earth Sciences and Engineering, Xi'an Shiyou University, Xi'an, Shaanxi 710065, China
[2] Shaanxi Key Lab of Petroleum Accumulation Geology, Xi'an Shiyou University, Xi'an, Shaanxi 710065, China
[3] Research Institute of Exploration and Development, PetroChina Qinghai Oilfield Company, Dunhuang 736200, China

Abstract

The Paleogene-Neogene lacustrine source rocks in the Mangai area of the Qaidam Basin are significant exploration targets. A comprehensive evaluation of four major intervals (E_3^2, N_1, N_2^1, N_2^2) was conducted through systematic organic geochemistry, maceral identification, thermal maturity analysis, and burial-thermal history modeling. Results show TOC contents of 0.203˜1.28% (avg. 0.74%), chloroform bitumen "A" of 0.0164˜0.2495% (avg. 0.132%), and total hydrocarbon contents of 69.29˜1637.48 μg/g (avg. 853.39 μg/g), indicating fair to good quality. Kerogen elemental analysis (H/C=0.97˜1.21), maceral composition (sapropelinite+exinite=70˜98%), and saturated hydrocarbon chromatography (dominant peaks at C17, C19, C21, C23) collectively indicate predominantly Type II_1 organic matter, with locally developed Type I. Thermal evolution exhibits distinct vertical zonation controlled by Neogene tectonic-thermal events: an immature-low maturity zone (R_0<0.7%) dominated by soluble organic matter degradation; a mature zone (R_0=0.7˜1.0%) with active kerogen cracking (HC/TOC up to 224.95%); and a high maturity zone (R_0>1.0%) characterized by gas generation via cracking. The saline to semi-saline reducing environment favored organic matter preservation, while mixed algal-terrestrial inputs (Type II_1) determined mainly oil-prone characteristics. The thick succession in the central depression, especially the Kaitemilike-Fenghuangtai region, shows the highest hydrocarbon potential. The mature zone (R_0=0.7˜1.0%) is optimal for conventional oil exploration, while the high maturity zone (R_0>1.0%) holds promise for natural gas. This multi-parameter study deepens the understanding of hydrocarbon generation mechanisms and provides an important case for evaluating Paleogene-Neogene lacustrine source rocks in the northern Tibetan Plateau.

Keywords: qaidam basin, mangai area, thermal evolution, paleogene to neogene, hydrocarbon source rocks.

Submitted: 30 December 2025
Accepted: 20 January 2026
Published: 08 February 2026

Vol. 2, **No.** 1, 2026.
10.62762/JGEE.2025.781750

***Corresponding author:**
Changan Shan
shanca@xsyu.edu.cn

Citation
Shi, S., Shan, C., Zhao, Z., Fei, Y., & Zhang, J. (2026). Organic Geochemical Characteristics and Thermal Evolution Characteristics of Paleogene to Neogene Source Rocks in Mangai Area, Qaidam Basin. *Journal of Geo-Energy and Environment*, 2(1), 56–72.

© 2026 by the Authors. Published by Institute of Central Computation and Knowledge. This is an open access article under the CC BY license (https://creativecommons.org/licenses/by/4.0/).

1 Introduction

After more than half a century of continuous exploration and development, the proven reserves and productivity of oil and gas resources in the Qaidam Basin still show a steady growth trend, indicating good resource potential [1]. The latest round of source rock prediction indicates that high-quality source rocks are developed in the Mangai area, characterized by high organic matter abundance (TOC > 1.0%), substantial thickness, and stable distribution, providing a material foundation for large-scale hydrocarbon generation [2]; meanwhile, the spatial structure of reservoirs in this area is complex.(pore-fracture dual media), and lithologic types are diverse (with clastic rocks and carbonate rocks coexist), forming good reservior-preservation combination conditions [3–5]. This geological background makes the western Qaidam area a key region with the most exploration potential in the basin.The Mangai area is affected by Neogene source rock development, and develops carbonate beach bar and terrigenous clastic beach bar reserviors as two types of high-quality natural gas reservoirs. High-quality hydrocarbon source rock and beach bar sand reservoirs are developed and have good source-reservoir-cap rock combination conditions, making it a favorable area for natural gas exploration in Qaidam Basin [6, 7]. During the Paleogene to Neogene period, structural activity was relatively strong in western Qaidam area, and a large number of fault structures were developed. Good trap conditions were formed in the late period, and mainly clastic rock and carbonate reservoir were developed. Spatially, effective gas source rocks were mainly distributed in the northwest Qaidam area and local area near the Mangai depression [8, 9]. The Mangai area was a salty lake basin reduction environment, and its organic matter type is mainly mixed type, using the geochemical parameter quantitative evaluation method to evaluate hydrocarbon source rocks in the northwest Qaidam Basin, it has been determined again that the upper member of the Lower Ganchaigou Formation and the Upper Ganchaigou Formation have higher organic matter abundance and are the dominant hydrocarbon source rocks [10]. Previous studies have systematically investigated the Cenozoic lacustrine fine-grained clastic reservoirs in the basin through integrated analytical approaches including core description, thin section analysis, X-ray diffraction (XRD), and scanning electron microscopy (SEM). These investigations have comprehensively characterized the sedimentological features, reservoir properties, and diagenetic evolution processes of the reservoirs, with particular emphasis on stage division of diagenesis. Notably, the formation mechanisms and controlling factors of two sets of high-quality fine-grained clastic reservoirs in both shallow and mid-deep intervals of the Mangai area were clarified for the first time. Further research combining sedimentary reservoir analysis with petroleum geology has provided in-depth understanding of the Paleogene-Neogene sedimentary facies distribution, hydrocarbon spatial distribution patterns, and reservoir formation dynamics in the western Qaidam Depression. These studies have innovatively proposed a "ring-belt distribution" accumulation model for hydrocarbons in this region, significantly advancing the understanding of hydrocarbon accumulation patterns in lacustrine basins [11–13]. While previous studies have made significant progress in understanding the sedimentary reservoir characteristics and hydrocarbon accumulation models of the basin, research on the quality of Paleogene–Neogene source rock samples in the Mangai area, particularly regarding organic matter type and thermal evolution degree, remains relatively limited and requires further in-depth investigation. Therefore, this study focuses on the Paleogene–Neogene source rocks in the Mangai area of the Qaidam Basin. Through systematic organic geochemical analysis of the source rock succession in this region, this study aims to: (1) Establish a multi-parameter comprehensive evaluation system to achieve refined characterization of organic matter abundance, type, and maturity; (2) Reveal the vertical zonation characteristics of source rock thermal evolution and its controlling mechanisms; (3) Clarify the controlling factors for the development of high-quality source rocks.

This research holds significant guiding importance for evaluating the geological conditions of hydrocarbon accumulation and sweet spot prediction in the study area, providing valuable references for the exploration and development of oil and gas resources in the Mangai area of the Qaidam Basin.

2 Geological setting

The Qaidam Basin is located in the northwest of Qinghai Province of China. It is surrounded by the Altun Mountains, the Kunlun Mountains and the Qilian Mountains in the northwest, southwest and northeast respectively. It is an inland basin with the highest altitude in China and one of the important oil and gas resource enrichment areas in

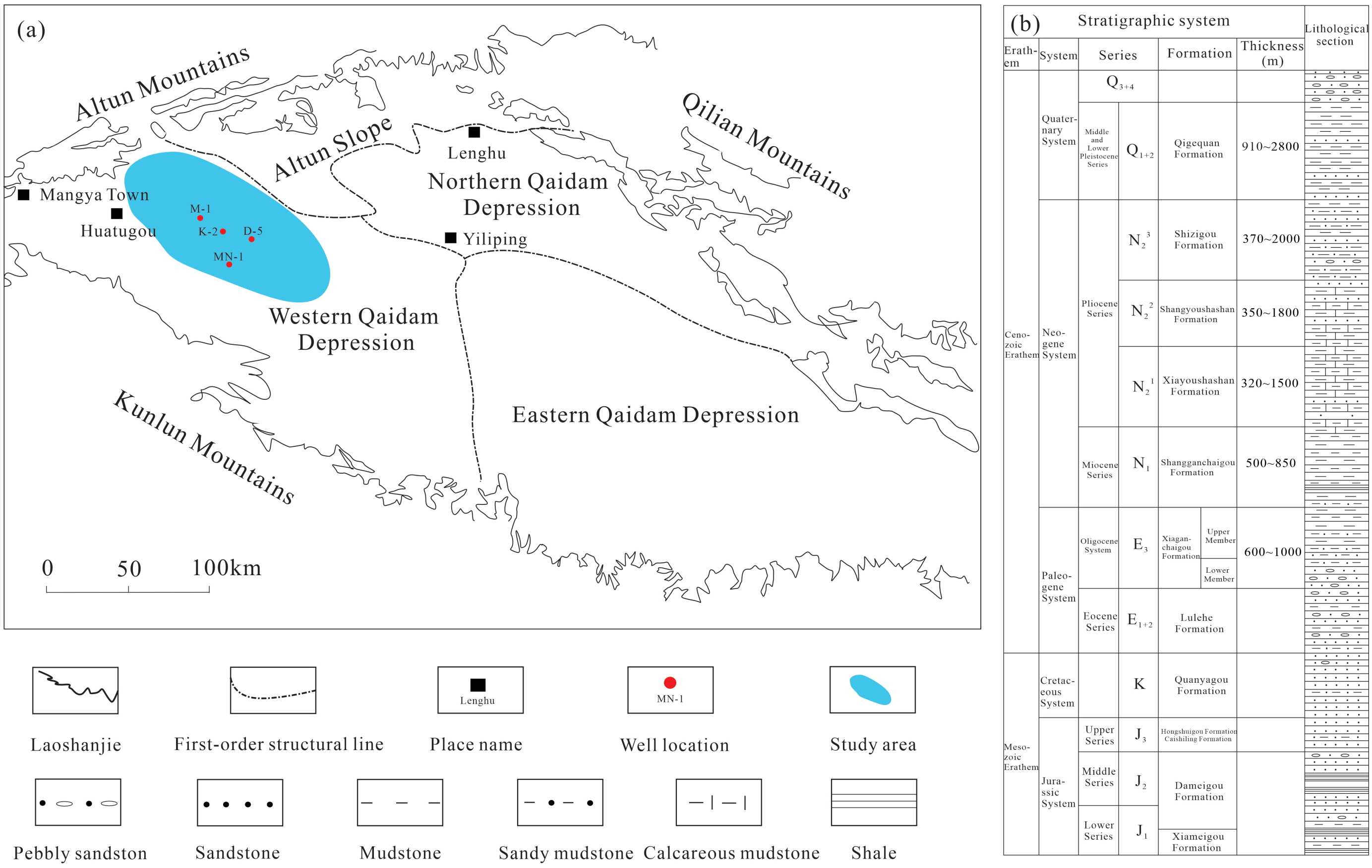

Figure 1. Location map (a) and composite stratigraphic column (b) of the Mangai area in the Qaidam Basin.

the western region of China [14–17]. The Mangai region is part of the western depression zone of the Qaidam Basin, located within the Mangai Depression (Figure 1(a)). The northeast part of the area is low and gentle, and the southwest part is high and steep. The mountain range is NW trending. The surface undulates violently. The structures such as Huangguamao, Mangai, Kaitemilike and Youdunzi are developed. The area is adjacent to Yingxiongling oil generating sag in the west, Mangai oil generating sag in the south, Youquanzi and Youdunzi in the north. Nanyishan and Dafengshan structures are closely connected to Dasaping minor structure and Fenghuangtai in the east. This area is composed of Shizigou-Youshashan structural belt, Youquanzi structural belt, Yingxiongling-Mangai depression, Nanyishan-Jianshishan structural belt and Luoyanshan structural belt. The overall structural strike is NW, and the structural axes are staggered and arranged in en echelon. It belongs to the Paleogene Neogene petroleum bearing system in the west of Qaidam Basin. The geological structural deformation is intense, and the sedimentary environment is special and complex. It has good oil reservoir structure [18–21].

The hydrocarbon source rocks in the Mangai region predominantly consist of lacustrine dark argillaceous rocks and carbonates (Figure 1(b)), exhibiting extensive lateral distribution and occurring across multiple stratigraphic intervals. Four principal source rock units have been identified (E_3^2, N_1, N_2^1, and N_2^2): The E_3^2 unit, composed primarily of thick gray to dark gray mudstone and silty mudstone, represents the most significant Paleogene-Neogene source rock system in the Qaidam Basin [22], with thickness varying from 200m to 1400m. The N_1 unit, characterized by dark gray mudstone and silty mudstone, shows relatively reduced thickness (300 900m). The N_2^1 unit, consisting of gray, light gray and dark gray calcareous mudstone and silty mudstone, with thickness varying from 500m to 900m, reaches maximum thickness in the Kaitemilike-Fenghuangtai area, while its overall distribution demonstrates an eastward migration trend, primarily concentrated in central and southern Mangai [7, 23–25]. The N_2^2 unit, dominated by gray to light gray calcareous mudstone and silty mudstone, varies in thickness from 200m to 2200m, with the thickest deposits occurring in the Kaitemilike-Fenghuangtai region.

Overall, lacustrine dark argillaceous rocks are developed throughout the interval from E_3^2 to N_2^2, characterized by fine-grained lithology, extensive lateral distribution, and considerable vertical thickness of the source rocks. The total thickness of dark mudstone accounts for over 80% of the stratigraphic thickness, with individual layers reaching a maximum of 27 m and typically ranging from 3 to 6 m. During the Paleogene–Neogene lacustrine basin evolution in this area, the E_3^2 period witnessed the most extensive basin extent, the deepest water column, high salinity, and prolific algal development, providing exceptional material foundation and preservation conditions for the formation of high-quality source rocks.

3 Samples and methods

3.1 Samples

In this study, mudstone samples were collected from four key coring wells (K-2, M-1, D-5, and MN-1) in the Paleogene-Neogene strata of the Mangai area, western Qaidam Basin. A systematic organic geochemical analysis was conducted, with a cumulative total of 1022 experimental samples. To ensure long-term preservation of sample freshness, all specimens were promptly and tightly wrapped with cling film and immediately transported to the laboratory for subsequent experiments.

3.2 Experiments

This study involved the analysis of 1022 shale core samples through systematic organic geochemical testing to comprehensively evaluate the organic matter abundance, type, and thermal evolution characteristics. A multi-parameter analytical approach was employed, including: Total Organic Carbon (TOC) determination (284 samples), chloroform bitumen "A" extraction (219 samples), Total Hydrocarbon (HC) content analysis (184 samples), kerogen elemental composition analysis (43 samples), kerogen maceral identification (38 samples), saturated hydrocarbon gas chromatography (189 samples), and vitrinite reflectance (R_0) measurement (67 samples). Based on the systematic experimental data and a comprehensive geochemical multi-index evaluation approach, this research reveals the organic geochemical characteristics and thermal evolution patterns of the Paleogene-Neogene hydrocarbon source rocks in the Mangai area of Qaidam Basin.

3.2.1 *Organic matter abundance analysis*

The TOC content was measured following the Chinese national standard GB/T19145 for total organic carbon analysis in sedimentary rocks. Approximately 0.3g of pulverized sample (200 mesh) was placed in a permeable crucible and treated with hydrochloric acid (1:7) for 12 hours to remove carbonate minerals (calcite and dolomite). The decarbonated sample was then combusted in a high-temperature oxygen stream, and the released CO2 was quantified using an infrared detector. TOC values were determined using a LECO CS-344 carbon/sulfur analyzer, with analytical precision controlled within $\pm 0.1\%$.

Chloroform bitumen "A" was extracted in accordance with the Chinese petroleum industry standard SY/T 5118-2005 using Soxhlet extraction. A 100 g aliquot of crushed rock sample was subjected to continuous extraction with analytical-grade chloroform at 65°C for 72 hours. The extract was concentrated by rotary evaporation and weighed to calculate the chloroform bitumen "A" content.

Total hydrocarbon content was determined using an Agilent 7890B gas chromatograph equipped with an HP-5MS capillary column (30m×0.25mm×0.25μm). The analytical conditions were as follows: injector temperature 300°C, detector temperature 320°C, and oven temperature programmed from 80°C (held for 2 min) to 310°C at 4°C/min (final hold for 20 min).

3.3 Organic matter type analysis

The elemental composition of kerogen was determined using a Vario EL III elemental analyzer. After removing inorganic minerals through HCl-HF treatment, the purified kerogen samples were subjected to high-temperature combustion to quantify carbon (C), hydrogen (H), and oxygen (O) contents. Atomic ratios of H/C and O/C were subsequently calculated. Each sample was analyzed in triplicate, with the mean values reported for final interpretation.

Maceral identification was performed in compliance with the Chinese petroleum industry standard SY/T 5125-2014 using a Leica DM4500P polarized light microscope. Under oil immersion at 500× magnification, a minimum of 500 points were randomly counted to determine the volumetric percentages of sapropelinite, exinite, vitrinite, and inertinite groups.

Biomarker analysis was conducted according to the Chinese national standard GB/T 18606-2017 for determining biomarkers in sediments and crude oils. A Thermo Scientific Trace 1310 GC coupled with an ISQ 7000 mass spectrometer was employed, equipped with an HP-5MS capillary column (60m×0.25mm×0.25μm).

The GC temperature program was initiated at 60°C, then ramped at 6°C/min to 260°C, followed by a slower ramp of 1.5°C/min to 320°C (held for 20 min). Ultra-high purity helium (99.999%) was used as carrier gas at a constant flow rate of 1 mL/min. The injector and transfer line temperatures were maintained at 300°C and 310°C, respectively.

3.4 Maturity analysis of organic matter

The vitrinite reflectance (R_0) was measured by using German Leitz MPV-SP microphotometer. The experimental process strictly followed SY/T5124-2012 standard: the core sample was made into 2.5cm×2.5cm×1.5cm optical sheet, which was coarsely ground, finely ground and polished to mirror surface; the sapphire standard sample was used (reflectance 0.589%); oil immersion objective (50×), 546nm monochromatic light, measurement temperature controlled at 23±1°C; at least 30 vitrinite particles are randomly measured for each sample, and the arithmetic mean value is taken as the final R_0 value after eliminating abnormal values; every 10 samples are inserted into the standard sample (GBW13403) for verification, and the relative error is controlled within ±0.02%.

4 Results and Discussion

As the material basis for hydrocarbon generation, the abundance, type, and maturity of organic matter in source rocks serve as the core indicators for assessing the petroleum resource potential of a basin [26–30]. This study, based on systematic geochemical analyses of the Paleogene–Neogene source rock succession in the Mangai area of the Qaidam Basin, focuses on the distribution characteristics and controlling factors of organic matter abundance and type. Through the integration of abundance indicators—such as total organic carbon (TOC), chloroform bitumen "A," and total hydrocarbons (HC)—with multi-parameter analytical methods including kerogen elemental composition, maceral analysis, and saturated hydrocarbon gas chromatography, the organic geochemical characteristics of the source rocks in the Mangai area are elucidated. By systematically comparing these findings with previous research, this study advances the quantitative evaluation of source rock geochemical parameters, refines the classification of thermal evolution stages, and enhances the understanding of controlling mechanisms. This section systematically elaborates the distribution patterns of organic matter abundance and type in the Mangai area and discusses their implications for petroleum geology.

4.1 Abundance of organic matter in source rocks

Organic matter in source rocks serves as the fundamental material basis for hydrocarbon generation, with its abundance directly determining the petroleum resource potential of sedimentary basins. In the organic geochemical assessment system for sedimentary rocks, total organic carbon (TOC), chloroform bitumen "A", and total hydrocarbon (HC) content constitute the core parameters for characterizing organic matter abundance. These indicators not only quantitatively reflect the hydrocarbon generation potential but also form the key geochemical basis for source rock classification [31–33]. Specifically, TOC represents

Table 1. Statistical table of organic matter abundance of hydrocarbon source rocks in Mangai area.

well	position	formation thickness(m)	dark mudstone thickness (m)	TOC(%)/ number of samples	"A"(%)/ number of samples	HC(μg/g) / number of samples	kerogen type
M-1	N_2^2	2062	1661	0.44/38	0.048/26	356.54/23	II
	N_2^1	998	950	0.45/21	0.074/12	585.34/7	II
	N_1	860	768	0.47/15	0.0438/10	328.5/8	II
	E_3^2	280	238	0.203/6	0.0626/3	383.68/1	III
K-2	N_2^2	2104	2032.5	0.57/47	0.0183/21	164.89/12	III
	N_2^1	940	882.5	0.79/18	0.0769/11	553.8/10	II
	N_1	913	818	0.61/32	0.0434/36	506.71/21	III
	E_3^2	269.5	259	1.28/7	0.2495/6	1637.48/6	I
D-5	N_2^2	338	320.5	0.2367/6	0.0271/6	195.182/6	III
	N_2^2	2032	1682	0.2601/14	0.0164/10	101.687/10	III
	N_2^1	707.16	554.16	0.6014/7	0.066/5	418.95/5	I
MN-1	N_2^2	1372	1112	0.36/24	0.015/24	69.29/24	no
	N_2^1	942	593	0.42/18	0.018/18	96.7859/18	III
	N_1	671	451	0.37/14	0.023/14	126.165/14	III
	E_3^2	895	571	0.44/17	0.04/17	288.03/17	II
total				284	219	182	

the enrichment degree of original organic matter, chloroform bitumen "A" reflects soluble organic matter content, and total HC directly indicates generated hydrocarbon abundance. Together, these parameters establish a comprehensive evaluation framework for source rock quality [34].

A total of 284 mudstone samples were analyzed for TOC, with 219 high-TOC samples subsequently subjected to chloroform bitumen "A" extraction, and 182 samples analyzed for HC content. The measured ranges and averages were: TOC (0.203~1.28%, avg. 0.74%), chloroform bitumen "A" (0.0164~0.2495%, avg. 0.132%), and total HC (69.29~1637.48μg/g, avg. 853.39μg/g)(Table 1).

As shown in Table 1, the organic matter abundance of Paleogene–Neogene source rocks in the Mangai area generally meets the criteria for fair-to-good source rock quality. Particularly, the E_3^2 interval in Well K-2 demonstrates superior geochemical properties, with an average TOC of 1.28%, chloroform bitumen "A" of 0.2495%, and total hydrocarbon (HC) content of 1637.48 μg/g, significantly exceeding other intervals and reaching the standard of a Type I high-quality source rock. The development of this high-quality source rock is controlled by the following factors:

(1) Strongly reducing saline lacustrine environment: During the deposition of the E_3^2 interval, the Mangai Depression was characterized by a persistently saline to semi-saline deep to semi-deep lake setting, with pronounced water column stratification and anoxic bottom conditions, which favored organic matter preservation.

(2) High algal productivity input: This period was marked by prolific algal blooms, reflected in the high proportion of sapropelinite in kerogen macerals, indicating that the hydrocarbon-generating organic matter was predominantly derived from aquatic lower organisms.

(3) Low terrigenous clastic dilution: Relatively high lake levels during this phase led to reduced terrigenous sediment input, thereby enhancing organic matter enrichment.

(4) Early diagenetic organic matter preservation: The interbedded development of carbonate rocks and mudstones, coupled with early diagenetic cementation, inhibited the degradation of organic matter.

Consequently, the E_3^2 interval not only exhibits high organic matter abundance but also excellent organic matter type (Type I), representing the most promising principal hydrocarbon-generating source rock unit in the Mangai area. Its formation results from the synergistic effects of sedimentary environment, biological productivity, and preservation conditions, providing significant insights for hydrocarbon resource assessment and exploration target selection in this region.

Following China's terrestrial source rock evaluation standard (SY/T 5735-2019), the classification criteria are: non-source rock (TOC<0.2%, bitumen<0.015%, HC<100 μg/g), poor (0.2%<TOC<0.4%, 0.015%< "A" <0.05%, 100μg/g <HC<200μg/g), fair (0.4%<TOC<0.6%, 0.1%< "A" <0.2%, 200μg/g <HC<500μg/g), and good source rocks (TOC>0.6%, 0.05%< "A"<0.1%, 500μg/g<HC<1000μg/g). Accordingly, the N_2^1 unit in Wells K-2 and D-5, and N_1~N_2^2 unit in Well M-1 qualify as fair source rocks, while the E_3^2 unit in Well K-2, deposited in a saline lacustrine reducing environment favorable for organic matter preservation, meets the criteria for good source rocks.

The results of organic matter abundance assessment in this study are generally consistent with the findings of Tian et al. [8] regarding the source rocks in the western Qaidam Basin, both indicating that the E_3^2 interval serves as the main source rock unit with the highest organic matter abundance. However, through statistical analysis with a larger sample size, this study further quantifies the distribution ranges and average values of TOC, chloroform bitumen "A," and total hydrocarbons (HC) across various intervals. It specifically demonstrates that the average TOC content of the E_3^2 interval in Well K-2 reaches 1.28%, meeting the criteria for Type I high-quality source rocks. This quantitative understanding provides a direct basis for the refined evaluation of the hydrocarbon generation potential of the source rocks.

4.2 Classification of organic matter types in source rocks

Differences in organic matter type are primarily reflected in chemical composition and maceral characteristics, which directly control the phase behavior of their thermal degradation products (oil vs. gas). The distribution patterns of organic matter types are mainly governed by original biological sources and depositional environment conditions, while also being influenced by the staged evolution of thermal maturity (R_0). The Paleogene–Neogene succession in the Mangai area

Table 2. Analysis and comparison of kerogen elements in Mangai area.

well	position	well section(m)	elemental composition (%)			atomic ratio		kerogen type	number of samples
			C	H	O	H/C	O/C		
K-2	N_2^2	350-2307	43.02	3.814	5.021	1.072	0.088	II_1	10
	N_2^1	3750	52.63	4.57	5.97	1.042	0.0851	II_1	1
	N_1	3850-4538	46.21	4.07	5.33	1.056	0.087	II_1	9
	E_3^2	4710-4960	52.13	4.62	5.98	1.063	0.086	II_1	3
MN-1	N_2^2	800-1150	45.94	4.58	15.68	1.21	0.26	II_1-II_2	3
	N_2^1	1700-2650	47.43	4.69	8.65	1.20	0.15	II_1	4
	N_1	2900-3250	54.78	4.42	6.79	0.97	0.09	II_1-II_2	3
	E_3^2	3612-4150	52.94	4.52	12.36	1.03	0.18	II_1-II_2	6
D-5	N_2^1	2504.5-3275	46.95	4.48	6.49	1.21	0.13	II_1	4
total									43

developed in a saline to semi-saline lacustrine setting, with organic matter derived from mixed inputs: on the one hand, algal and planktonic productivity flourished in deep to semi-deep lake environments, contributing hydrogen-rich components; on the other hand, terrestrial higher plants from surrounding uplifted areas were introduced through fluvial systems, supplying oxygen-rich components. This mixing of aquatic and terrestrial organic matter is the primary reason for the dominance of Type II_1 (sapropelic–humic) organic matter in the source rocks of this area. In local deep depressions, such as the Kaitemilike–Fenghuangtai area, algal inputs are overwhelmingly dominant, resulting in Type I high-quality source rocks. For organic matter typing, this study employs an integrated classification scheme combining kerogen elemental analysis (H/C, O/C atomic ratios), maceral identification, and saturated hydrocarbon gas chromatography. Focusing on mudstone and marl intervals within the Paleogene–Neogene succession, systematic geochemical analysis is conducted to reveal the distribution patterns of organic matter types and their implications for hydrocarbon generation.

4.3 Classification by kerogen element

Carbon, hydrogen and oxygen are the most important elements in organic matter and kerogen [35, 36]. The elemental composition of kerogen reflects not only the nature of organic matter, but also the evolution degree of organic matter. Therefore, using the elemental analysis of kerogen, along with the change of element relative content, H/C atomic ratio and O/C atomic ratio, is one of the widely used methods to determine the type of kerogen. 43 kerogen element samples were selected from the samples with high TOC content in three coring wells of Well K-2, Well MN-1 and Well D-5 in Mangai area (Table 2). The results show that the kerogen elements C, H and O contents in N_2^2~E_3^2 layers of Well K-2 and Well MN-1 are relatively low, with C element ranging from 43.02% to 54.78%, with an average value of 49.39%, H element ranging from 3.814% to 4.69%, with an average value of 4.41%. The atomic ratios of H/C and O/C have a narrow range, for example, H/C atomic ratio is between 0.97~1.21, with an average value of 1.08, while O/C atomic ratio is between 0.0851~0.26, with an average value of 0.128, indicating that kerogen (II_1) is mainly humus-sapropelic. The data points of 23 sample layers of Well K-2 are plotted on the H/C-O/C atomic ratio relation diagram. From the N_2^2~E_3^2 four-layer superposition diagram, it can be seen that the positions of each layer of Well K-2 are concentrated in the area of mixed type (Figure 2).

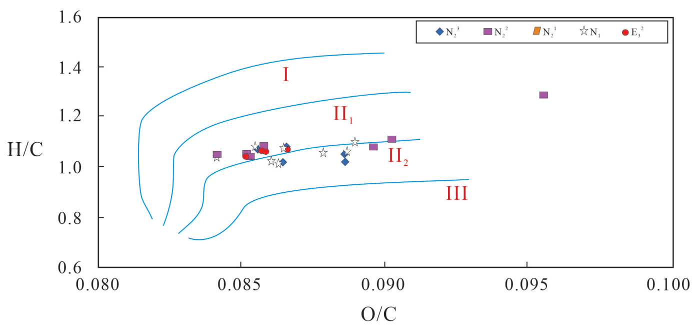

Figure 2. Classification diagram of kerogen elemental composition (H/C vs. O/C atomic ratios) for Well K-2.

4.3.1 *Classification by kerogen maceral*

The kerogen macerals consist of four primary components: sapropelinite, exinite, vitrinite, and inertinite. Microscopic examination of these macerals was conducted to determine their relative abundances for organic matter typing. This study analyzed 38

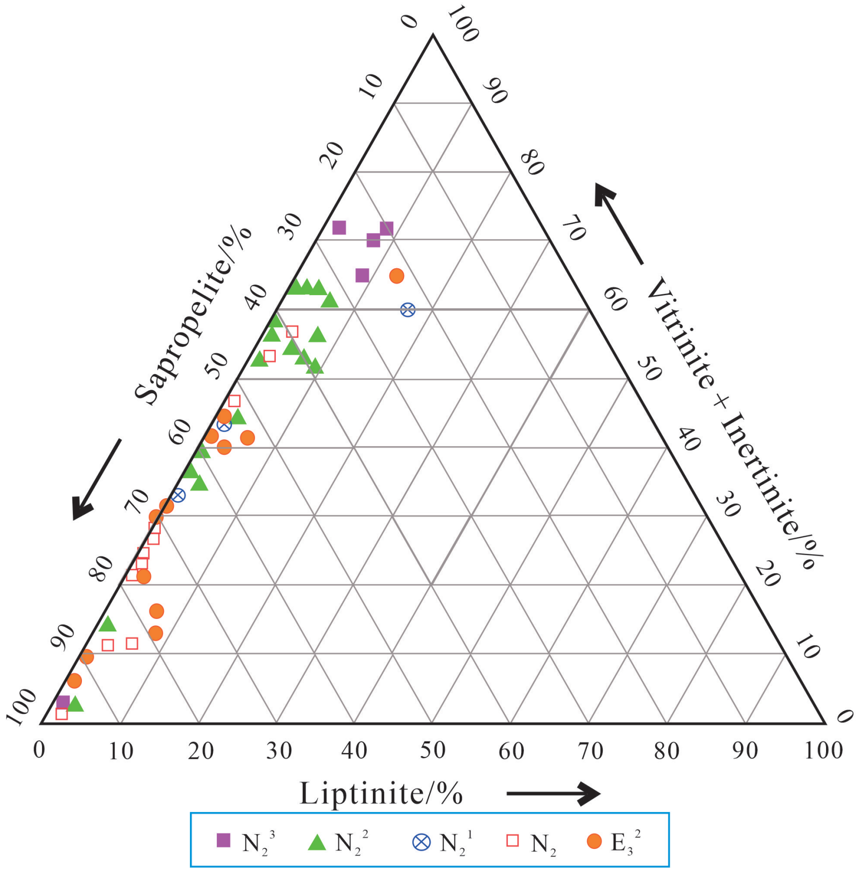

Figure 3. Ternary diagram of kerogen maceral composition for Well K-2 source rocks.

high-TOC mudstone core samples from wells K-2 and MN-1. Results reveal that in K-2 well's source rock, sapropelinite dominates (58.04%), primarily as amorphous sapropelinite of algal and planktonic origin with frequent acritarch occurrences. Exinite occurs minimally (3.09%), mainly as sporinite, cutinite and suberinite. Vitrinite constitutes 35.13%, while inertinite is scarce (3.74%)(Figure 3). These findings demonstrate that K-2 source rocks formed from mixed algal/planktonic/benthic materials with hydrogen-rich higher plant components.

The maceral composition analysis of Paleogene-Neogene source rocks in Well MN-1 (Table 3) reveals that the N_2^2~E_3^2 oil-prone source intervals are dominated by hydrocarbon-generating components, particularly algal-derived liptinites. The kerogen assemblage is characterized by exceptionally high percentages of sapropelic constituents (sapropelinite+exinite=70.21~87.96%), with minimal inertinite and vitrinite content. This composition indicates superior kerogen quality, classified as Type I (sapropelic) and Type II_1 (sapropelic-humic) organic matter, which demonstrates excellent oil-generation potential. The predominance of algal-derived macerals suggests deposition in anoxic, nutrient-rich lacustrine environments favorable for the preservation of hydrogen-rich organic matter. These geochemical characteristics confirm the N_2^2~E_3^2 interval as a highly efficient petroleum source rock in the study area.

4.3.2 Gas chromatographic classification by saturated hydrocarbons

Saturated hydrocarbon gas chromatography analysis can be used to determine the biogenic composition and evolution degree of hydrocarbons. For example, the main peak carbon of n-alkanes with a rear peak in the rear peak type of C25~C33, reflecting that the original organic matter is imported from terrestrial higher plants; a front peak in the range of C15~C19 reflects that the source material is derived from aquatic lower organisms; and the bimodal type reflects that the mother material has mixed sources of lower organisms and higher plants. According to the chromatographic characteristics of saturated hydrocarbon from 189 samples from 4 coring wells in the area of Mangai, the peak types are mainly single peak type and double peak type, and the main peak carbon is mainly C17, C19, C21 and C23 (Figure 4), which obviously belongs to the

Table 3. Statistics of source rock maceral components of Well MN-1.

well	position	well section(m)	vitrinite	inertinite	exinite	phycozoite	chitinite + sapropelite	TI
MN-1	N_2^2	800-1650	17.49	3.07	6.78	72.66	79.44	59.87
	N_2^1	1699-2650	8.6	3.44	2.99	84.97	87.96	76.57
	N1	2900-3300	21.91	7.88	4.69	65.52	70.21	43.56
	E_3^2	3350-4200	12.86	2.9	4.58	79.68	84.26	69.41

distribution characteristics of II_1-II_2 organic matter. This result is consistent with the analysis of kerogen element and kerogen microcomponent identification (indicating a predominance of humic-sapropelic type), collectively indicating that the organic matter type of source rocks in the study area is mainly type II (humus-sapropelic mixed type), and locally enriched type II (sapropelic type).

By integrating multiple indicators including kerogen elemental composition, maceral analysis, and saturated hydrocarbon chromatography, this study has determined that the organic matter in the source rocks of the Mangai area is predominantly Type II_1, with locally developed Type I. This understanding is more systematic than previous research, particularly through quantitative maceral statistics, which reveal that the sapropelinite content in high-quality source rocks from Well MN-1 can reach up to 87.96%. This finding elucidates the formation mechanism of high-quality source rocks from the perspective of biological source composition.

4.4 Characteristics of thermal evolution of hydrocarbon source rocks

The thermal evolution characteristics of hydrocarbon source rocks are key indicators for evaluating hydrocarbon generation potential and hydrocarbon generation process, and their evolution process is mainly controlled by geological factors such as organic matter type, thermal maturity and burial history [37]. Previous studies on thermal evolution in the western Qaidam Basin have primarily focused on identifying “effective gas source rocks” with $R_0 \geq 0.8\%$ [8], while insufficient attention has been given to the complete thermal evolution sequence and its controlling mechanisms. This study, through systematic analysis of parameters such as vitrinite reflectance (R_0), carbon preference index (CPI), and odd-even predominance (OEP), combined with burial-thermal history modeling, establishes for the first time a vertical thermal evolution zonation model for source rocks in the Mangai area and reveals the controlling role of tectonic-thermal events on the thermal evolution process.

The Mangai area is located in the western part of the Qaidam Basin. Since the Cenozoic, it has experienced multiple phases of tectonic subsidence and uplift, with an overall high paleo-geothermal gradient (3.0~3.5°C/100 m), providing sustained thermal dynamic conditions for the thermal evolution of source rocks. Based on the burial-thermal history modeling results of Well K-2 (Figure 5), combined with regional tectonic evolution analysis, it is shown that the thermal evolution of source rocks in the Mangai Depression exhibits distinct stages: the E_3^2 source rocks began rapid burial during the late Paleogene (approximately 30~25 Ma), entered the hydrocarbon generation window ($R_0 \geq 0.7\%$) in the early Neogene (approximately 20~15 Ma), and reached the mature to highly mature stage (R_0 = 0.7~1.2%) in the middle to late Neogene (approximately 10~5 Ma). This burial-thermal history process is closely related to basin subsidence-sedimentary responses induced by regional tectonic activities, such as strike-slip movement along the Altun Fault and uplift of the Kunlun Mountains.

At present, the evaluation system for thermal evolution degree of hydrocarbon source rocks has been relatively well-developed, and commonly used maturity parameters include vitrinite reflectance (R_0) and rock pyrolysis parameters.(e.g. Tmax, HI, PI) and biomarker compounds (such as sterane, hopane isomerization index), etc. In addition, carbon dominance index (CPI) and parity dominance (OEP) of n-alkanes, as organic geochemical indicators, have significant response to thermal evolution degree, so they can also be used as auxiliary evaluation parameters [38]. By selecting key exploration wells in the Mangai area, and systematically measuring key parameters such as vitrinite reflectance (R_0), carbon preference index (CPI)

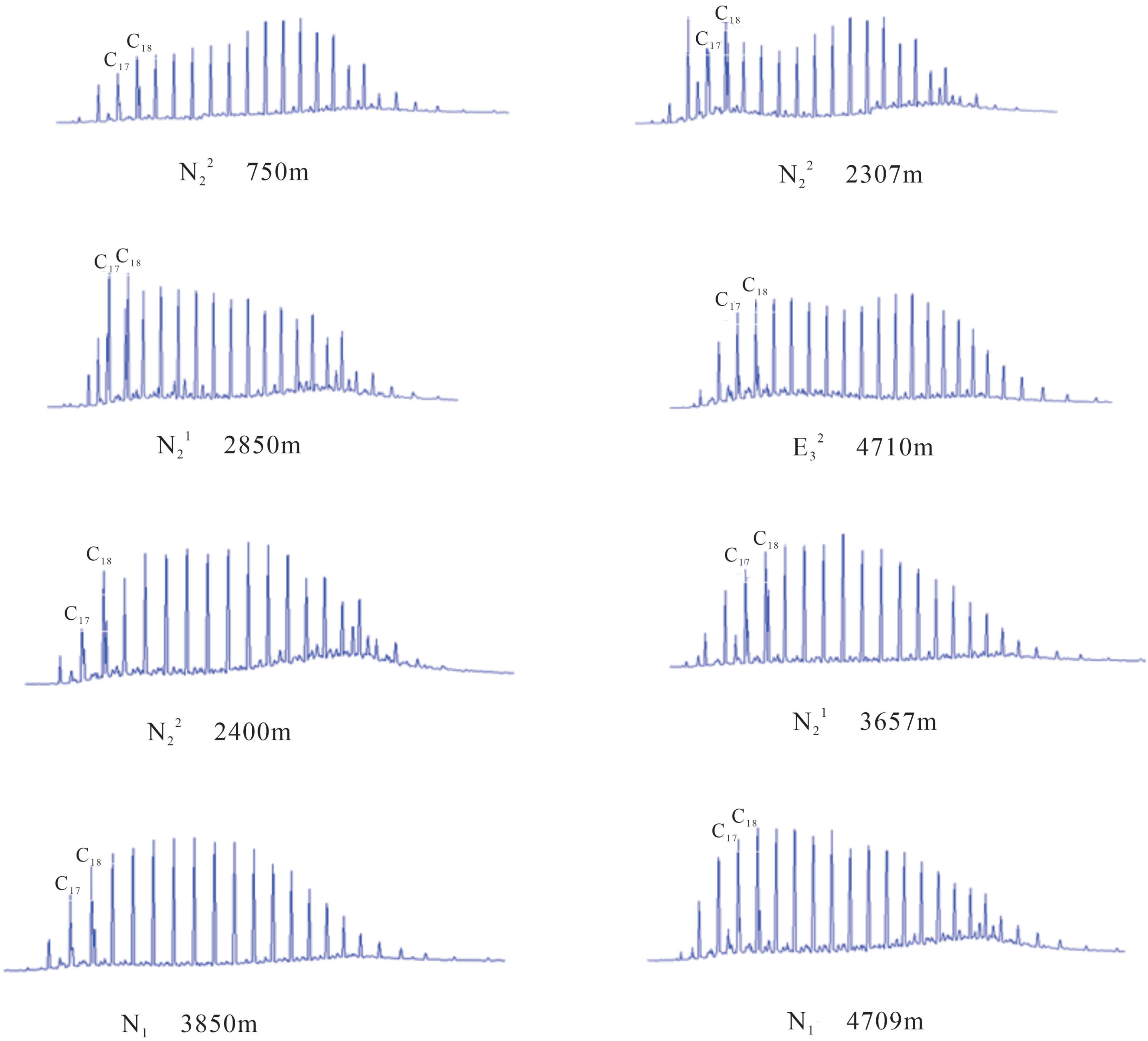

Figure 4. Typical saturated hydrocarbon gas chromatogram for Well K-2 source rocks.

and odd-even predominance (OEP) in combination with regional geological background, this study comprehensively analyzes and quantitatively evaluates the thermal evolution of Paleogene to Neogene hydrocarbon source rocks.

The results indicate that the vertical zonation of thermal evolution parameters (Figures 6 and 7) closely corresponds to the burial-thermal history. In the shallow section of Well D-5 (depth < 3085 m), the source rocks exhibit typical immature characteristics: chloroform bitumen "A," total hydrocarbon (HC) content, and transformation ratios (A/TOC, HC/TOC) decrease with depth, non-hydrocarbon content increases, OEP and CPI values show significant fluctuations (>1.5), and vitrinite reflectance (R_0) is less than 0.5%, indicating that the organic matter has not yet entered the effective hydrocarbon generation stage. In the interval below 3085 m, the source rocks display low-maturity features: "A" and HC contents, as well as transformation ratios, gradually increase with depth; OEP and CPI values approach 1 (average 1.1~1.2); and R_0 rises to 0.51%, indicating that the organic matter has entered the early thermal degradation stage and begun generating immature to low-maturity hydrocarbons (Figure 6).

The thermal evolution profile of Well MN-1 further

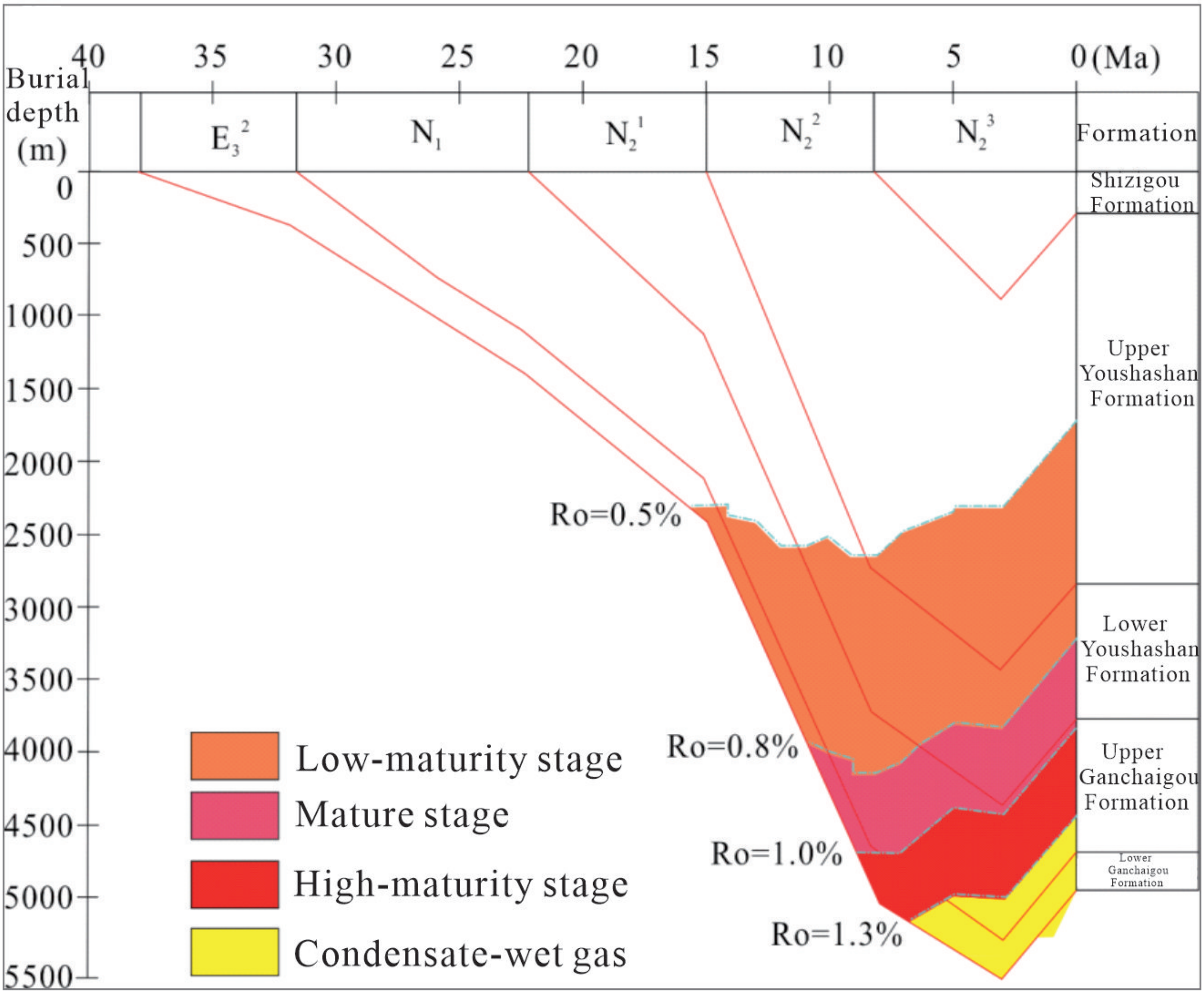

Figure 5. Integrated burial and thermal evolution history diagram for Well K-2.

reveals a continuous depth-dependent trend of maturity (Figure 7). In the shallow section (depth < 1900 m), the immature source rocks show relatively stable but gradually decreasing "A" and HC contents, increasing non-hydrocarbon proportions, OEP and CPI > 1, Tmax < 430°C, and R_0 = 0.41˜0.65%. In the 1900˜3450 m interval, the source rocks enter the mature stage: "A" and HC contents and transformation ratios increase significantly (HC/C rises from 0.01 to 0.057), OEP and CPI ≈ 1, Tmax > 430°C (approaching 440°C), and R_0 = 0.61˜1.05%, indicating oil generation window characteristics dominated by kerogen thermal degradation. Notably, below 3450 m, HC/C increases sharply to 0.161, non-hydrocarbon content decreases, and R_0 = 1.01˜1.15%, marking the transition of the source rocks into the high-maturity stage, where they begin generating substantial amounts of condensate and wet gas.

The analytical results from Well K-2 provide significant insights into regional hydrocarbon generation mechanisms. In the shallow section (<2400m, $R_0 \leq 0.79\%$), the immature to low mature hydrocarbon source rocks consist of saltwater to brackish lacustrine facies higher plant derivatives "A"/TOC=4.03%, HC/TOC=10.40%, indicating a hydrocarbon generation mechanism of direct degradation of soluble organic matter. These rocks are composed of saltwater to brackish lacustrine facies higher plant derivatives. However, in the deep section (depth>2400m, $R_0 \geq 0.8\%$), mature hydrocarbon source rocks show "A"/TOC=15.17%,

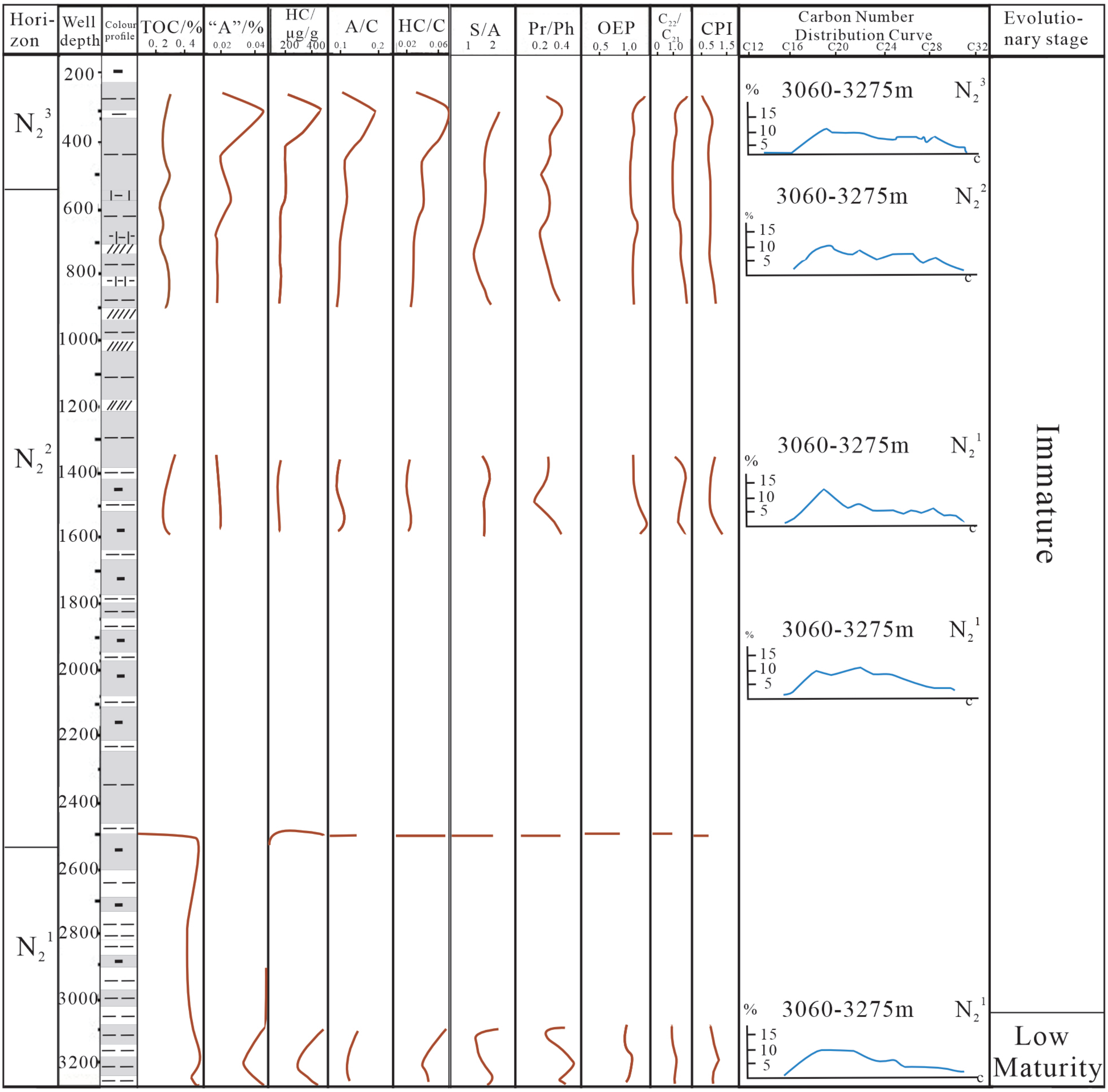

Figure 6. Vertical evolution profile of geochemical parameters for source rocks in Well D-5, Paleogene–Neogene, Mangai area.

HC/TOC=224.95%, indicating that kerogen thermal degradation has become the main hydrocarbon generation mechanism and the source rocks have entered the peak period of hydrocarbon generation (Table 4). These rocks are mainly contributed by algae, microorganisms and bacteria.

Notably, the abundant salt minerals in source rocks under saline lacustrine conditions may have catalyzed the pyrolysis of organic matter, further accelerating hydrocarbon generation and cracking. Therefore, the thermal evolution zonation of source rocks in the Mangai area is not merely a function of burial depth and time but also a result of the combined effects of tectonic–thermal events, sedimentary infilling, and fluid–rock interactions.

Based on the above analysis, we have established a thermal evolution model for the source rocks in the Mangai area (Figure 8): The immature to low-maturity zone (R_0 < 0.7%) is dominated by hydrocarbon

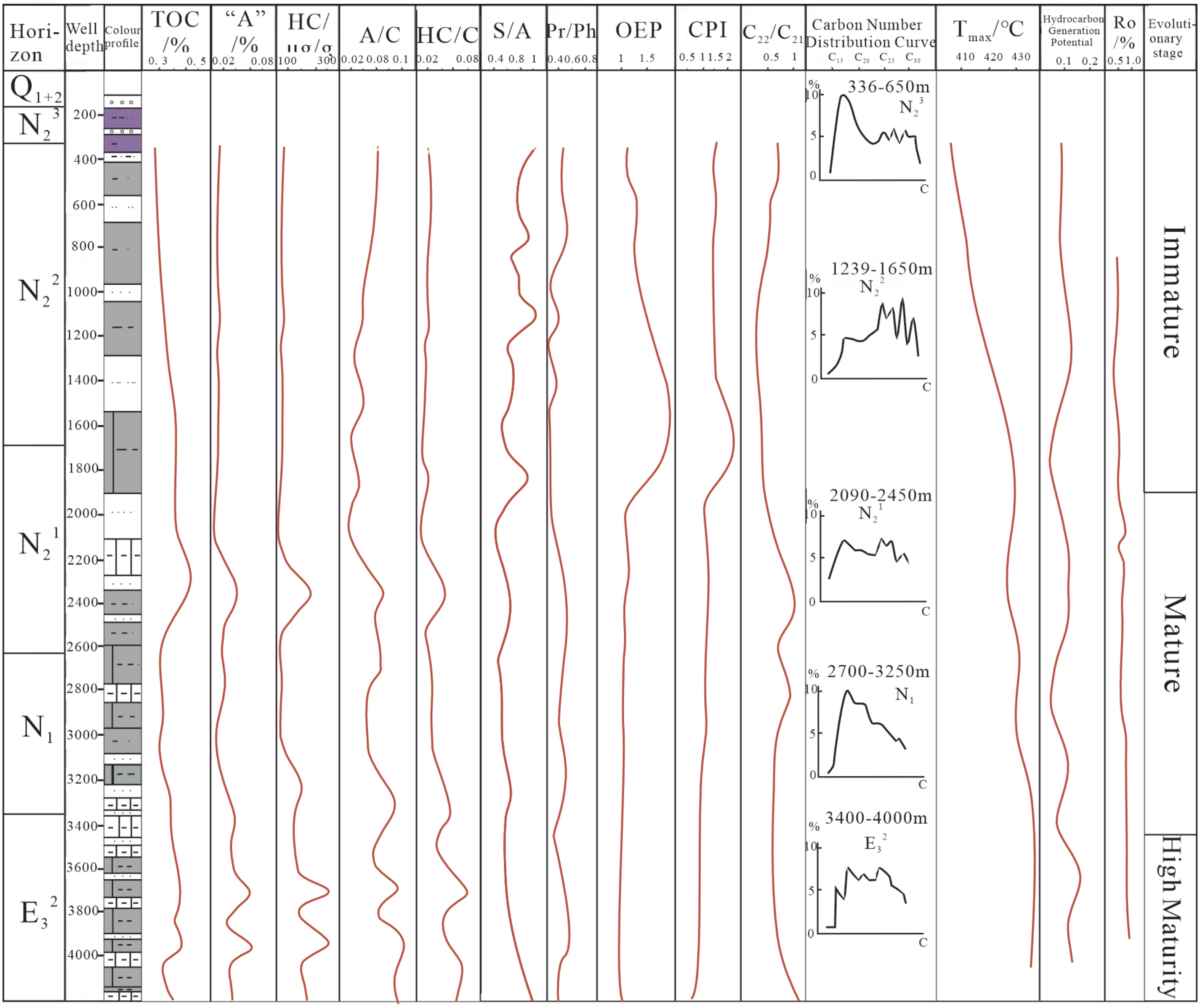

Figure 7. Vertical evolution profile of geochemical parameters for source rocks in Well MN-1, Paleogene–Neogene, Mangai area.

Table 4. Organic Matter Conversion Rate in Different Oil and Gas Generation Zones of Well K-2.

hydrocarbon belt	TOC(%)/ number of samples	"A"(%)/ number of samples	HC(μg/g)/ number of samples	"A"/TOC(%)/ number of samples	HC/TOC(%)/ number of samples
low maturity hydrocarbon generation zone	0.53/53	0.0182/21	134.26/9	4.03/21	10.4/9
mature hydrocarbon generation zone	0.72/66	0.0866/49	684.07/41	15.17/49	224.95/41

generation from soluble organic matter, influenced by inputs of higher plant materials. The mature zone (R_0 = 0.7~1.0%) is characterized by kerogen thermal degradation, with increasing contributions from algal precursors, maximizing oil generation potential. The high-maturity zone (R_0 > 1.0%) is dominated by gas generation via cracking, accompanied by a reduction in non-hydrocarbon content, reflecting the terminal stage of organic matter evolution.

This understanding provides an important theoretical basis for predicting hydrocarbon resource distribution and selecting exploration directions in the region. Specifically, the mature zone (R_0 = 0.7~1.0%), corresponding to the peak oil generation window, represents a favorable target for conventional oil exploration. In contrast, the high-maturity zone (R_0 > 1.0%) is characterized by gas generation via cracking and holds potential for natural gas exploration.

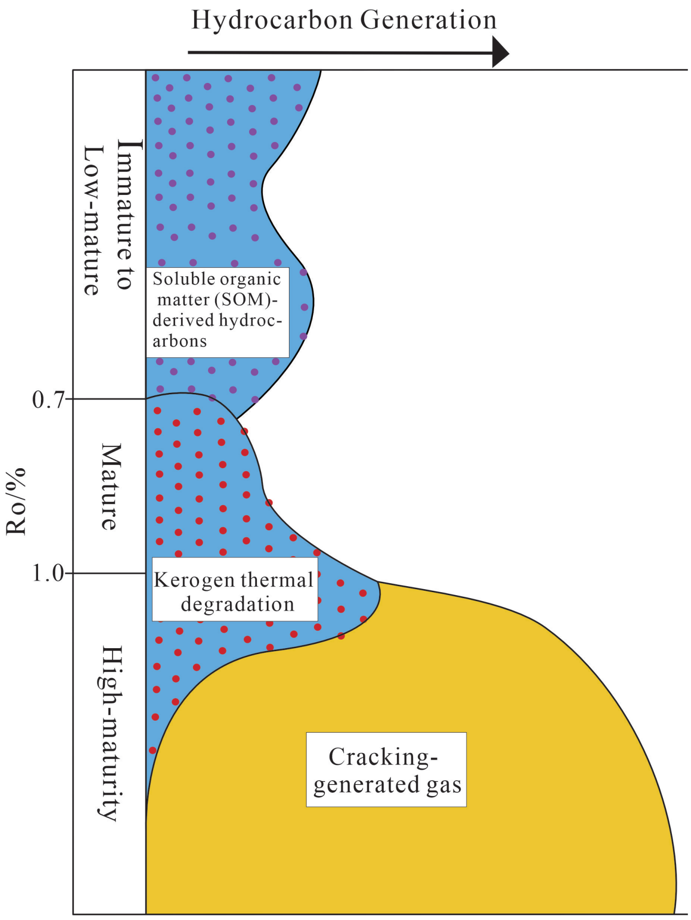

Figure 8. Comprehensive hydrocarbon generation model diagram for Paleogene–Neogene source rocks in the Mangai area [39].

5 Conclusions

(1) Four sets of major hydrocarbon source rocks (E_3^2, N_1, N_2^1, N_2^2) developed in the Paleogene-Neogene of the Mangai area, dominated by deep to semi-deep lacustrine dark mudstones and carbonates. These rocks are characterized by wide distribution, large thickness (single layers up to 27 m, cumulative thickness 200~2200 m), and moderate to high organic matter abundance. The E_3^2 source rocks, with average TOC of 1.28%, chloroform bitumen "A" of 0.2495%, and total hydrocarbons of 1637.48 μg/g, meet the criteria for Type I good source rocks, representing the regional principal oil-generating interval. The high organic matter abundance is attributed to the coupled effects of a strongly reducing saline lacustrine environment, high algal productivity, low clastic dilution, and favorable early diagenetic preservation conditions.

(2) Comprehensive geochemical characterization, including kerogen elemental analysis (H/C atomic ratios ranging 0.97~1.21), maceral composition (sapropelinite + exinite content 70~98%), and saturated hydrocarbon chromatographic profiles (dominated by front-peaked unimodal and bimodal distributions with primary n-alkane peaks at C17, C19, C21, and C23), collectively indicates that the organic matter is predominantly Type II_1 (sapropelic-humic) with localized development of Type I (algal-rich) kerogen. Notably, the high-quality source rocks in the MM-1 well area exhibit exceptionally high sapropelinite content (up to 87.96%), demonstrating superior hydrocarbon generation potential with strong oil-prone characteristics.

(3) The Paleogene to Neogene source rocks in Mangai area of Qaidam Basin exhibit a wide range of quality from poor to high. The kerogen type is mainly II_1type, with a small amount of I type and II_2type. The organic matter in the source rocks is of mixed type. The E_3^2-N_2^1 source rock intervals have high organic matter abundance and good source material type, while the E_3^2 source rock has organic matter abundance high enough to reach type I kerogen standard, which is the main source rock formation in Mangai area and has great potential for oil and gas exploration and development.

(4) A complete vertical thermal evolution zonation model for the source rocks in the Mangai area is established: an immature-low maturity zone (R_0<0.7%) dominated by soluble organic matter degradation; a mature zone (R_0=0.7~1.0%) where kerogen thermal degradation prevails, corresponding to the peak liquid hydrocarbon generation window; and a high maturity zone (R_0>1.0%) characterized by gas generation via cracking. This evolution is controlled by the burial and heating history driven by regional tectonic-thermal events since the Neogene, such as the strike-slip movement along the Altun Fault and the uplift of the Kunlun Mountains.

Data Availability Statement

Data will be made available on request.

Funding

This work was supported without any funding.

Conflicts of Interest

Ze Zhao is affiliated with the Research Institute of Exploration and Development, PetroChina Qinghai Oilfield Company, Dunhuang 736200, China. The authors declare that this affiliation had no influence on the study design, data collection, analysis, interpretation, or the decision to publish, and that no other competing interests exist.

AI Use Statement

The authors declare that no generative AI was used in the preparation of this manuscript.

Ethical Approval and Consent to Participate

Not applicable.

References

[1] Wei, X., Sha, W., Shen, X., Si, D., Zhang, G., Ren, S., & Yang, M. (2021). Petroleum exploration history and enlightenment in Qaidam Basin. *Xinjiang Petroleum Geology, 42*(3), 302-311. [CrossRef]

[2] Feng, D., Liu, C., Tian, J., Xie, M., Huo, H., Yang, T., ... & He, Y. (2025). Key Controlling Factors of Hydrocarbon Accumulation of Fine-Grained Mixed Sequence in a Saline Lacustrine Basin: An Integrated Research of Petroleum System in the Northwestern Qaidam Basin, Qinghai–Tibet Plateau. *Natural Resources Research*, 1-26. [CrossRef]

[3] Yang, Y., Qiu, L., Wan, M., Jia, X., Cao, Y., Lei, D., & Qu, C. (2019). Depositional model for a salinized lacustrine basin: The permian Lucaogou formation, Jimsar sag, Junggar Basin, NW China. *Journal of Asian Earth Sciences, 178*, 81-95. [CrossRef]

[4] Yang, H. A. N., Xian-zhi, G. A. O., Fei, Z. H. O. U., Bo, W. A. N. G., Jun, Z. H. U., & Li-feng, D. U. A. N. (2020). Thermal evolution of Jurassic source rocks and their impact on hydrocarbon accumulation in the northern margin of Qaidam Basin, NW China. *Natural Gas Geoscience, 31*(3). [CrossRef]

[5] Chen, Z., Wang, B., Liu, Z., Zhou, F., Yi, L., Shao, Z., ... & Zhang, H. (2025). Late accumulation characteristics of hydrocarbon in the Cenozoic of the western Qaidam Basin: The hydrocarbon accumulation effect of the Tibetan Plateau uplift. *Chinese Journal of Geology, 60*(4), 1176-1191.

[6] Guo, Z., Ma, Y., Yi, S., Tian, J., Zeng, X., Kong, H., & Wang, Y. (2017). Simulation and exploration direction of Paleogene-Neogene gas system in the western Qaidam Basin. *Natural Gas Geoscience, 28*(1), 82-92. [CrossRef]

[7] Zhanguo, L. I. U., Chao, Z. H. U., Senming, L. I., Jianqin, X. U. E., Qingshun, G. O. N. G., Yanqing, W. A. N. G., ... & Guangyong, S. O. N. G. (2017). Geological features and exploration fields of tight oil in the Cenozoic of western Qaidam Basin, NW China. *Petroleum Exploration and Development, 44*(2), 217-225. [CrossRef]

[8] Tian, J., Dong, Q., & Liu, J. (2021). Analysis on accumulation conditions and target optimization of Paleogene - Neogene gas reservoirs in Western Qaidam Basin. *Special Oil & Gas Reservoir, 28*(1), 26-33.

[9] Liu, C., Li, H., Zhang, X., Zheng, S., Zhang, L., Guo, Z., ... & Zeng, X. (2016). Geochemical characteristics of the Paleogene and Neogene saline lacustrine source rocks in the western Qaidam Basin, northwestern China. *Energy & Fuels, 30*(6), 4537-4549. [CrossRef]

[10] Wanxin, H. A. O., Fei, Z. H. O. U., Guo, C. H. E. N., Guojie, S. U. I., Yaohui, X. U., & Hui, T. I. A. N. (2023). Geochemical characteristics and their differential responses to formation mechanisms of the Paleogene and Neogene source rocks in western Qaidam Basin. *Natural Gas Geoscience, 34*(10), 1855-1870. [CrossRef]

[11] Li, W., Hu, D., Gong, C., Fan, T., Chen, Y., Li, Y. N., ... & Leng, Q. (2024). Controlling factors of high-quality reservoirs in low permeability sandstone: a case study of the upper member of the lower Ganchaigou formation, Qaidam basin. *Frontiers in Earth Science, 12*, 1396061. [CrossRef]

[12] Guoyong, L. I. U., Jianqin, X. U. E., Songtao, W. U., Kunyu, W. U., Haoting, X. I. N. G., Peng, P. A. N. G., & Chao, Z. H. U. (2024). Petroleum geology and ring-shaped distribution of the Paleogene-Neogene hydrocarbon resources in western Qaidam Depression, Qaidam Basin. *Oil & Gas Geology, 45*(4), 1007-1017. [CrossRef]

[13] Guoyong, L. I. U., Songtao, W. U., Kunyu, W. U., Yue, S. H. E. N., Gang, L. E. I., Haoting, X. I. N. G., & Guoxin, L. I. (2024). Characteristics and hydrocarbon accumulation model of Paleogene whole petroleum system in western depression of Qaidam Basin, NW China. *Petroleum Exploration and Development, 51*(5), 1097-1108. [CrossRef]

[14] Lin, C., Wu, C., Guan, X., Elias, J., Ren, C., & Zhang, W. (2025). Sedimentology and sequence stratigraphy of strike-slip fault-controlled continental lakes: Insights from the SW Qaidam Basin, NE Tibetan Plateau. *Sedimentary Geology, 486*, 106913. [CrossRef]

[15] Yin, J., Zhang, S., Lu, X., Wu, Z., Hui, G., & Ju, Y. (2019). Controls of the Altyn Tagh Fault on the Early–Middle Miocene sedimentation in the Honggouzi Area, Qaidam Basin, Western China. *Journal of Asian Earth Sciences, 181*, 103908. [CrossRef]

[16] Daowei, Z. H. A. N. G., Dade, M. A., Yan, C. H. E. N., Kunyu, W. U., Zhihong, C. A. I., Jian, Z. H. A. O., & Jiangong, W. A. N. G (2019). Research progress on oil and gas geology and exploration practice in Qaidam Basin. *Xinjiang Petroleum Geology, 40*(5), 1. [CrossRef]

[17] Meng, B., Zhou, S., & Li, J. (2024). Geochemical characteristics and significance of molecular markers in the Paleogene-Neogene crude oils of the Northwest Qaidam Basin. *ACS Omega, 9*(41), 42361-42374. [CrossRef]

[18] Guoxin, L. I., Rukai, Z., Yan, C. H. E. N., Jingwei, C. U. I., Kunyu, W. U., Chenggang, X. I. A. N., & He, L. I. U (2022). Geological characteristics, evaluation criteria and discovery significance of Paleogene Yingxiongling shale oil in Qaidam Basin, NW China. *Petroleum Exploration and Development, 49*(1), 21-36. [CrossRef]

[19] Li, X., Wu, K., Wang, J., Yang, S., Zhang, Q., & Zhang, Q. (2022). Impact of lithologic heterogeneity on brittleness of cenozoic unconventional reservoirs (Fine-Grained) in western Qaidam Basin. *Minerals, 12*(11), 1443. [CrossRef]

[20] Qinghua, W. A. N. G., Haijun, Y. A. N. G., & Wei, Y. A. N. G. (2025). New progress and future exploration targets in petroleum geological research of ultra-deep clastic rocks in Kuqa Depression, Tarim Basin, NW China. *Petroleum Exploration and Development, 52*(1), 79-94. [CrossRef]

[21] Guangyong, S. O. N. G., Zhanguo, L. I. U., Yanqing, W. A. N. G., Guohui, L. O. N. G., Chao, Z. H. U., Senming, L. I., ... & Qingshun, G. O. N. G. (2024). Lithofacies types, sedimentary cycles, and facies models of saline lacustrine hybrid sedimentary rocks: A case study of Neogene in Fengxi area, Qaidam Basin, NW China. *Petroleum Exploration and Development, 51*(6), 1507-1520. [CrossRef]

[22] Changhao, Z. H. A. N. G., Xin, F. U., Lianliang, Z. H. A. N. G., Hongzhen, D. U. A. N., Qiang, L. I., & Wei, Z. H. A. N. G. (2023). Characteristics of source rocks in the upper member of lower Ganchaigou formation in Ganchaigou area, Qaidam basin. *Mud Logging Engineering, 34*(2), 139-144.

[23] Huang, C., Chang, H., Cui, J., Li, Y., Lu, Y., Li, X., ... & Wu, L. (2017). Oilgocene sedimentary characteristics and hydrocarbon accumulation model in the western Qaidam Basin. *Acta Petrolei Sinica, 38*(11), 1230-1243. [CrossRef]

[24] Wang, J., Zhang, D., Yang, S., Li, X., Shi, Y., Cui, J., ... & Chang, H. (2020). Sedimentary characteristics and genesis of the salt lake with the upper member of the Lower Ganchaigou Formation from Yingxi sag, Qaidam basin. *Marine and Petroleum Geology, 111*, 135-155. [CrossRef]

[25] Yi, F., Yi, H., Mu, C., Tang, W., Li, N., Chen, Y., ... & Xia, G. (2023). Organic geochemical characteristics and organic matter accumulation of the Eocene lacustrine source rock in the Yingxi area, Western Qaidam Basin, China. *International Journal of Earth Sciences, 112*(4), 1277-1292. [CrossRef]

[26] Wang, B., Chen, M., Tian, H., Sun, J., Liu, L., Liang, X., ... & Qu, Z. (2025). Geochemical characteristics and genetic origin of tight sandstone gas in the Daning–Jixian Block, Ordos Basin. *Processes, 13*(12), 4019. [CrossRef]

[27] Bai, J., Qian, K., Wu, X., Dou, X., & He, Y. (2025). Thermal cracking for upgrading medium-low maturity shale oil: evolution of organic matter occurrence. *Scientific Reports, 15*(1), 43054. [CrossRef]

[28] Xu, Q. N., Zhu, Y. M., Chen, S. B., Liu, Y., Wang, X. Q., Shang, F. H., & George, S. C. (2025). Illitisation impeded the thermal evolution of extractable organic matter: An interpretation of the mineralogy and thermal maturation of early Cambrian source rocks in Yunnan Province, China. *Petroleum Science*. [CrossRef]

[29] Zhu, L., Wang, Z., Wang, F., & Tian, Y. (2025). Discussion on influencing factors of hydrocarbon generation in deep source rocks: A case study of Bozhong Sag, Bohai Bay basin. *Unconventional Resources, 6*, 100166. [CrossRef]

[30] Zhang, M., Zhu, X., Ji, W., Lin, X., & Ye, L. (2025). Effect of sedimentary environment on mudrock lithofacies and organic matter enrichment in a freshwater lacustrine basin: Insight from the Triassic Chang 7 Member in the Ordos Basin, China. *Sustainability, 17*(22), 10248. [CrossRef]

[31] Zeng, B., Qu, J., Mi, Z., Xie, E., Fu, H., Yang, S., ... & Li, M. (2025). The control of effective source rocks on the distribution of hydrocarbon reservoirs in a lacustrine rift-basin: insights from a 3D basin modeling study. *Journal of Petroleum Exploration and Production Technology, 15*(2), 21. [CrossRef]

[32] Liu, Q., Zhang, L., Chen, Z., Han, G., Fu, X., Teng, J., & Wang, Y. (2024). Exploring the prospects of deep natural gas resources from the geochemical parameters of the Shahejie Formation source rocks in the Banqiao depression. *Natural Gas Industry B, 11*(4), 443-453. [CrossRef]

[33] Zhao, Y., Huang, C., Chen, F., & Yue, Q. (2025). Hydrocarbon generation potential and geochemical characteristics comparison of source rocks in the Southwestern Qaidam basin, China. *Scientific Reports, 15*(1), 8281. [CrossRef]

[34] Chen, Y., Han, Y., Zhang, P., Wang, M., Qiu, Y., Zhu, X., & Zhang, X. (2023). Comparison of Evaporite-Related Source Rocks and Implications for Petroleum Exploration: A Case Study of the Dongying Depression, Bohai Bay Basin, Eastern China. *Energies, 16*(13), 5000. [CrossRef]

[35] Xiaodong, W. A. N. G., Bo, W. A. N. G., Jilei, Y. A. N. G., Peng, H. A. O., & Kuo, L. I. (2025). Kinetics of hydrocarbon generation of different types of organic matter in the KL-A structure of the Bohai Bay Basin. *Natural Gas Geoscience, 36*(2), 354-366. [CrossRef]

[36] Cai, C., Cai, J., Du, J., Lei, T., Wang, X., & Li, Z. (2023). Multistage Hydrocarbon Generation of Saline Lacustrine Source Rocks in Hydrous Pyrolysis: Insights from Clay Mineral–Organic Matter Interactions. *ACS omega, 8*(16), 14710-14729. [CrossRef]

[37] Wang, Y., Zhang, X., Wang, E., Zhang, J., Li, Q., & Sun, G. (2005). 40Ar/39Ar thermochronological evidence for formation and Mesozoic evolution of the northern-central segment of the Altyn Tagh fault system in the northern Tibetan Plateau. *Geological Society of America Bulletin, 117*(9-10), 1336-1346. [CrossRef]

[38] Feng, D., Liu, C., Tian, J., Xie, M., Huo, H., Yang, T., ... & He, Y. (2025). Key Controlling Factors of Hydrocarbon Accumulation of Fine-Grained Mixed Sequence in a

Saline Lacustrine Basin: An Integrated Research of Petroleum System in the Northwestern Qaidam Basin, Qinghai–Tibet Plateau. *Natural Resources Research*, 1-26. [CrossRef]

[39] Guoxin, L. I., Rukai, Z., Yan, C. H. E. N., Jingwei, C. U. I., Kunyu, W. U., Chenggang, X. I. A. N., & He, L. I. U. (2022). Geological characteristics, evaluation criteria and discovery significance of Paleogene Yingxiongling shale oil in Qaidam Basin, NW China. *Petroleum Exploration and Development*, *49*(1), 21-36. [CrossRef]

Shiling Shi received the B.Eng. degree in Electrical Engineering and Automation from Henan University of Engineering, Zhengzhou 451191, China, in 2023. (Email: sslty1999@163.com)

Changan Shan received the Ph.D. degree in Mineral Resource Prospecting and Exploration from Southwest Petroleum University, Chengdu 610500, China, in 2016. (Email: shanca@xsyu.edu.cn)

Ze Zhao received the M.S. degree in Structural Geology from Southwest Petroleum University, Chengdu 610500, China, in 2013. (Email: zzyjyqh@petrochina.com.cn)

Yue Fei received the B.Eng. degree in Cost Engineering from Shandong Jianzhu University, Jinan 250101, China, in 2023. (Email: 2408546819@qq.com)

Jiaqi Zhang received the B.S. degree in Resource Exploration Engineering from Xi'an Shiyou University, Dalian 710000, China, in 2023. (Email: 1983268791@qq.com)